Available online at www.sciencedirect.com
SCIENCE DIRECT®

Journal of the European Ceramic Society 24 (2004) 1031–1035
www.elsevier.com/locate/jeurceramsoc

Effect of sintering atmosphere on densification and dielectric characteristics in $Sr_{0.5}Ba_{0.5}Nb_2O_6$ ceramics

Shin-Il Kang[a], Joon-Hyung Lee[a], Jeong-Joo Kim[a], Hee Young Lee[b], Sang-Hee Cho[a,*]

[a]*Department of Inorganic Materials Engineering, Kyungpook National University, Daegu 702-701, South Korea*
[b]*Department of Materials Science and Engineering, Yeungnam University, Gyeongsan 712-749, South Korea*

Abstract

Ferroelectric $Sr_{0.5}Ba_{0.5}Nb_2O_6$ ceramics with a tetragonal tungsten bronze structure were sintered in an atmosphere with a different oxygen partial pressure (Po_2). The densification and diffuse phase transition (DPT) behaviors of the ceramics were examined. The density of the sintered body increased as the Po_2 of the sintering atmosphere increased, and the optical transmittance and the dielectric constant increased accordingly. However, the Curie temperature decreased. It is explained from a viewpoint of the internal stress on the sample, which is dependent on the porosity.

Keywords: Dielectric properties; Microstructure-final; SBN; Sintering; (Sr; Ba)Nb_2O_6; Tungsten bronze

1. Introduction

$Sr_xBa_{1-x}Nb_2O_6$ (SBN, where $0.25 \leqslant x \leqslant 0.75$) ceramics, and ferroelectric materials with tungsten bronze structures, have large pyroelectric[1] and linear electro-optic coefficients,[2] as well as strong photo refractive effects.[3] Piezoelectric properties with large spontaneous polarization of this material is of great interest because there were no volatilization problems, which has been one of the major problems in lead-based perovskite materials.[2]

The tungsten bronze structure consists of a skeletal framework of MO_6 octahedra, sharing corners to form three different types of tunnels parallel to the c-axis in the unit cell formula of $[(A1)_2(A2)_4C_4][(B1)_2(B2)_8]O_{30}$.[4] In the unit cell formula, both a 12-coordinated A1 site and a 15-coordinated A2 site exist, corresponding to four-fold and five-fold tunnels, respectively. The 9-coordinated C-site has the smallest space among the three different types of tunnels created by the framework of octahedra. Because of partial disorder of Ba^{+2} and Sr^{+2} ions filling partially the pentagonal and tetragonal sites, SBN reveals a relaxor-type diffuse phase transition.

The physical properties of materials are generally decided by the compositions of the materials.[5] However, the properties can be changed by processing parameters such as sintering temperature, time, sintering atmosphere, etc.[6,7] In SBN ceramics, the Curie temperature is a function of composition. The Curie temperature increases as the Sr/Ba ratio decreases. This characteristic is similar to perovskite structured $BaTiO_3$ ceramics, in which its Curie temperature increases as the Sr/Ba ratio decreases. When the composition is fixed, the Curie temperature of $BaTiO_3$ can be changed by external or internal stress since the tetragonality of $BaTiO_3$ is a function of the Curie temperature.

In tungsten bronze structured ceramics, the variation of Curie temperature by internal stress has been reported in ($PbBaNb_2O_6$) PBN ceramics.[8] When sintering temperature, one of the processing parameters, is changed, microstructure of the PBN ceramics was changed. Different grain size, porosity and development of cracks influenced the relief of internal stress, which resulted in the variation of Curie temperature of PBN.[8] On the other hand, the variation of dielectric constant and Curie temperature in SBN ceramics was reported by controlling sintering conditions and the degree of order–disorder.[9,10]

In this study, tungsten bronze structured SBN ceramics were sintered in different atmospheres with different oxygen partial pressures (Po_2). Microstructure development and dielectric characteristics were examined. Sintered density (porosity) of SBN ceramics was

* Corresponding author. Tel.: +82-53-950-5632; fax: +82-53-950-5645.
E-mail address: shcho@knu.ac.kr (S.-Hee Cho).

0955-2219/03/$ - see front matter © 2003 Elsevier Ltd. All rights reserved.
doi:10.1016/S0955-2219(03)00422-9

dependent on the Po_2. The maximum dielectric constant and Curie temperature of SBN ceramics were changed when the Po_2 of the sintering atmosphere changed. This can be explained through the densification and internal stress of SBN ceramics.

2. Experimental

A starting powder of $Sr_{0.5}Ba_{0.5}Nb_2O_6$ was prepared using high purity raw materials of $SrCO_3$(99.8%), $BaCO_3$(99.9%) and Nb_2O_5(99.9%) by the general solid state reaction process. The weighed powders were wet mixed and milled for 24 h in a plastic jar with zirconia balls and ethanol. After drying, the powder was calcined at 1300 °C for 6 h, then ball milled again for 24 h for crushing. Green pellets of 10 mm diameter disks were cold isostatic pressed at a pressure of 100 MPa for 3 min.

Samples were sintered at 1350 °C for 2 h after pre-sintering at 1250 °C for 2 h with a heating rate of 5 °C/min. This sintering method, which is called the dual-stage sintering method, is employed to avoid the generation of abnormal grain growth.[11] During sintering the oxygen partial pressure of the atmosphere was changed from 0 to 1 with an interval of 0.2 by changing oxygen (99.9%) and nitrogen (99.9%) flow rates. The nitrogen gas contained 10^{-3} atm residual oxygen. However, because the interval of Po_2 was wide, oxygen, air, nitrogen atmosphere were considered as $Po_2 \approx 1$, 0.2 and 0 atm, respectively.

The density of sintered samples was determined by the Archimedes method and the microstructure of polished samples was observed using a scanning electron microscope (SEM; Jeol, JML5400, Tokyo, Japan). The average grain size of the sample was determined by linear intercept method[12] on the SEM photographs. Wavelength dependent absorption and transmission of the SBN samples were measured by a UV–vis-NIR spectrophotometer (Varian, CARY 5G, Australia).

An Ag electrode was screen-printed on the both surfaces of sintered specimens, and fired at 600 °C for 10 min. Electrical conductivity of the sample was measured using a four-point resistance/resistivity measurement system (Changmin, CMT-SR1000N, Korea). Dielectric properties were analyzed by an impedance gain phase analyzer (HP4194A, USA) with a frequency increment in steps from 1 kHz to 1 MHz as a function of temperature. Internal stress of the samples was measured by micro-indentation method (Microindent, Matsuzawa, MXT-CX7E, Japan).

3. Results and discussion

Fig. 1 shows SEM micrographs of samples sintered at 1350 °C for 3 h in different Po_2 atmospheres. The mean grain size of the samples was (a)11.3 ± 1.7 μm, (b)10.2 ± 1.8 μm, (c)10.0 ± 2.0 μm, (d)11.4 ± 2.2 μm, (e)11.3 ± 1.3 μm, and (f)11.1 ± 2.1 μm. All of the samples showed a homogeneous microstructure and grain size distribution.

Fig. 2 shows relative density and mean grain size of sintered samples. The X-ray density of SBN (5.3297 g/cm^3) was considered as a theoretical density. The relative density of the sintered SBN increased slowly from 93.00 ± 0.26 to 96.64 ± 0.09% when the Po_2 of sintering atmosphere increased from 0 to 1 atm. However, mean grain size was almost invariant independently of the Po_2 as observed in Fig. 1. The increased relative density of the samples with respect to the Po_2 is due to oxygen gas entrapped in closed pores. In sintering powder compacts, atmosphere gases are important in the development of the final microstructures of the compacts. The final microstructures depend on the solubility of gases in the compacts. Insoluble gases limit pore shrinkage while soluble gas, like oxygen, in a closed pore can diffuse out during sintering, and eventually eliminate the closed pore.[13]

Optical transmittance of samples sintered in oxygen, air, and nitrogen gas in the visible light wavelengths (380–770 nm) is shown in Fig. 3. The thickness of the samples was 0.7 ± 0.02 mm. The transmittance of the sample sintered in oxygen ($Po_2 \approx 1$ atm) was highest roughly over 80%, while that of the sample sintered in air ($Po_2 \approx 0.2$ atm) was around 40%. However, the sample sintered in nitrogen ($Po_2 \approx 0$ atm) was opaque. When oxides are sintered in a lower Po_2 atmosphere, oxygen vacancies are produced which is the origin of free electrons.[14] It is well known that free electrons turn the transparent oxides to an opaque body because free electrons create new energy levels that absorb light.[15] The resistivity of the samples drastically decreased from 2063 to 917, and to 83 MΩ/cm^2 when the samples were sintered in oxygen, air, and nitrogen, respectively. Light scattering by pores in the sample seemed to partly contribute to the opaque characteristic.

Fig. 4 shows the dielectric characteristics of samples as functions of temperature and frequency. In Fig. 4(a) and (b), when the samples were sintered in oxygen and air, respectively, the dielectric constant showed frequency dependence below the phase transformation temperature. This characteristic is called ferroelectric relaxor behavior, where the phase transformation temperature increased, but the maximum dielectric constant decreased as the frequency increased.[16] Because, the Sr^{2+}, Ba^{2+} and vacancies in A sites are randomly distributed, SBN exhibits a DPT phenomena.[17] In Fig. 4(c), when the sample is sintered in nitrogen, anomalously huge dielectric constant (1×10^6 at 1 kHz, 2.2×10^5 at 1 MHz) and loss (~70% at 1 kHz, (~50% at 1 MHz) was observed. The dielectric anomaly is believed to be caused by the free electrons in the sample.

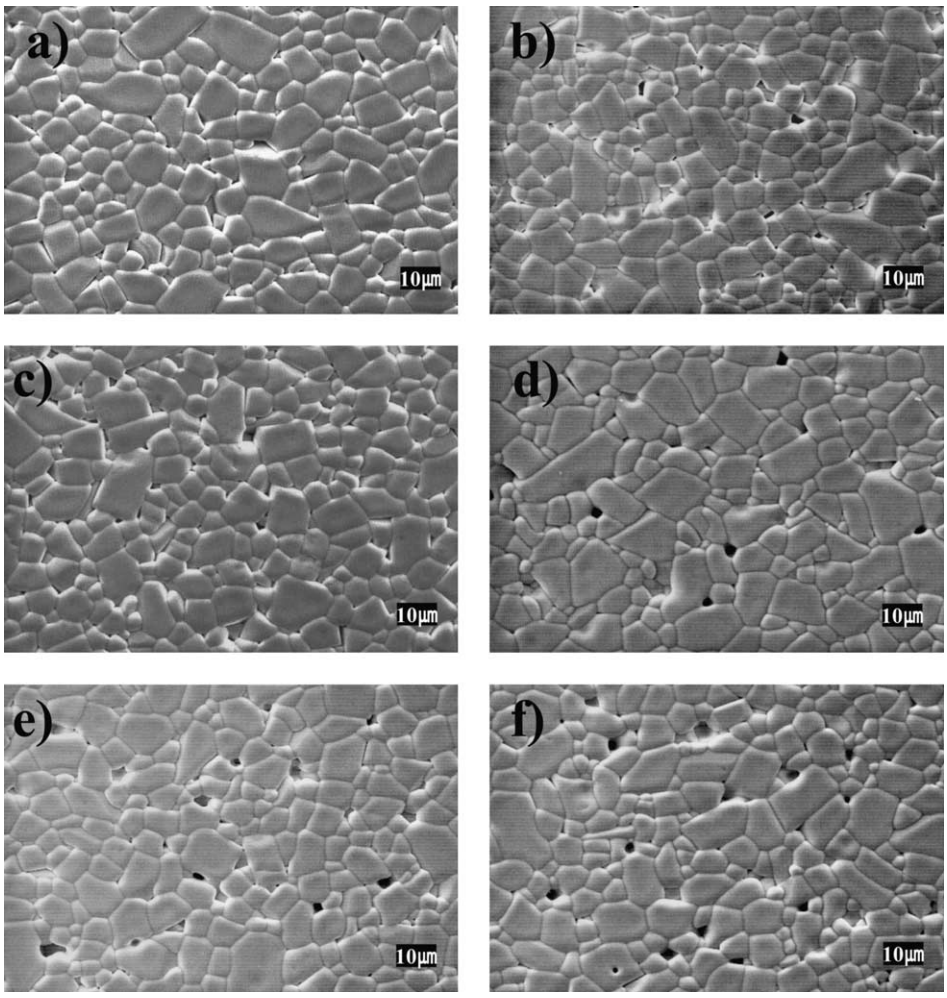

Fig. 1. Microstructures of samples sintered at 1350 °C for 2 h in different Po_2. (a) $Po_2 = 1$, (b) $Po_2 = 0.8$, (c) $Po_2 = 0.6$, (d) $Po_2 = 0.4$, (e) $Po_2 = 0.2$ and (f) $Po_2 \approx 0.0$.

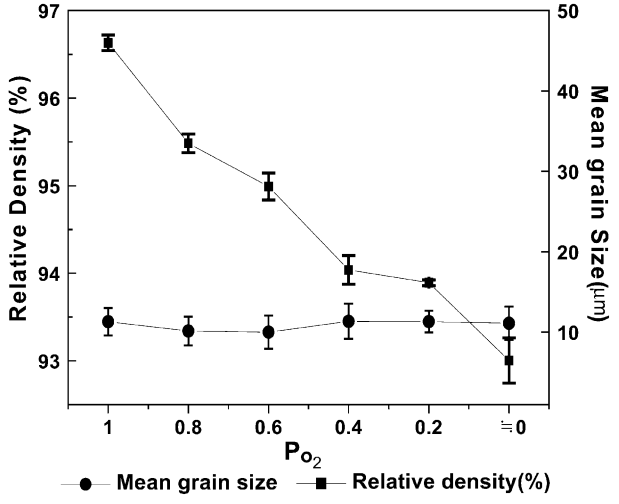

Fig. 2. Relative density and mean grain size of samples sintered at 1350 °C for 2 h in different PO_2.

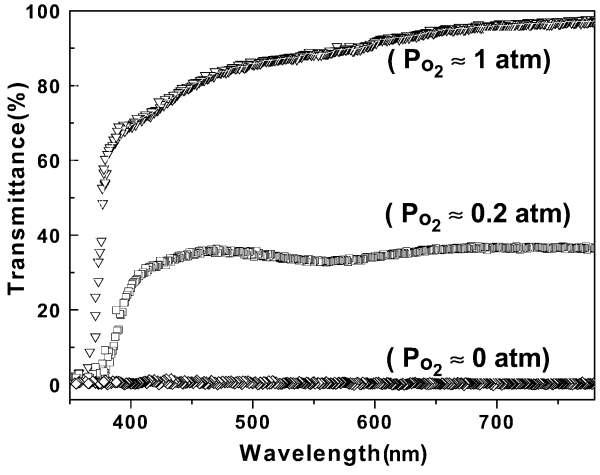

Fig. 3. Optical transmittance in visible light wavelength for the samples sintered in different Po_2 atmosphere.

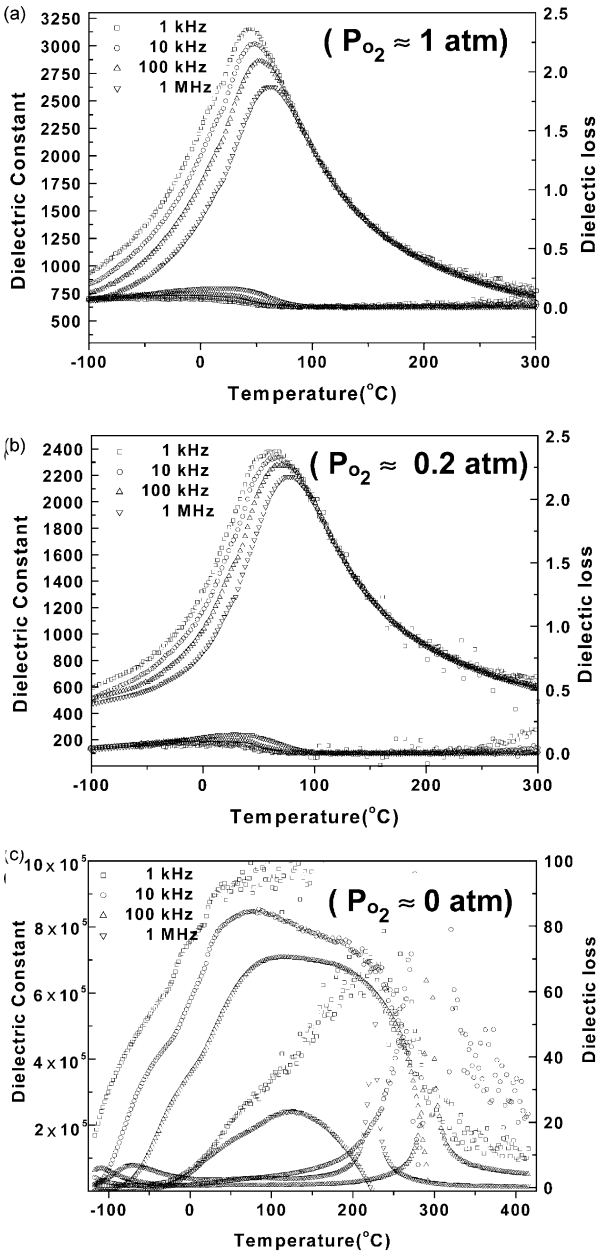

Fig. 4. Temperature dependence of dielectric constant and dielectric loss at different frequency for the samples sintered at 1350 °C for 2 h in different Po_2 atmosphere.

Fig. 5 shows the frequency dependence of the maximum dielectric constant for the samples sintered in different Po_2. The maximum dielectric constant of 3170 at 1 kHz was marked for the sample sintered in $Po_2 \approx 1$ atm, while that of 2364 was marked for the sample sintered in $Po_2 \approx 0.2$ atm. It is revealed that higher Po_2 leads to a higher maximum dielectric constant, which is caused by the increased density of the sintered body.

The phase transformation temperature of the samples as functions of Po_2 and frequency is presented in Fig. 6. The phase transformation temperature of the sample sintered in $Po_2 \approx 0.2$ atm was 77.4 °C at 1 kHz, while

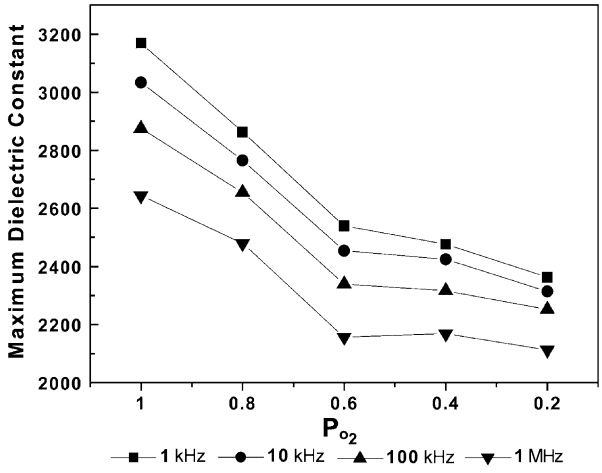

Fig. 5. Maximum dielectric constant vs. Po_2 as a function of frequency.

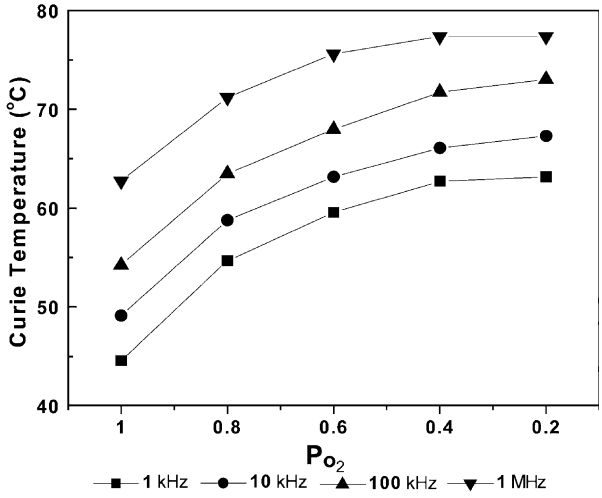

Fig. 6. Curie temperature vs. Po_2 as a function of frequency.

that of the sample sintered in $Po_2 \approx 1$ atm was 63.2 °C at 1 kHz, showing a tendency that the phase transformation temperature increases as the Po_2 increases.

In order to examine a cause of the phase transformation temperature change, the microindentation method was employed for a measurement of the internal stress of the samples.[18] A relationship between fracture toughness, applied load and internal stress can be expressed by;

$$K_{IC} = 0.0726 \times P/c^{3/2}$$

$$K_{IC} = K_{IC}^{o} + 2\delta_i[c/\pi]^{0.5}$$

K_{IC} : fracture toughness — P : applied load
K_{IC}^{o} : intrinsic fracture toughness — c : crack length
δ_i : internal stress

From the equations above, a relation between K_{IC} and $[c/\pi]^{0.5}$ can be achieved for the cases of samples

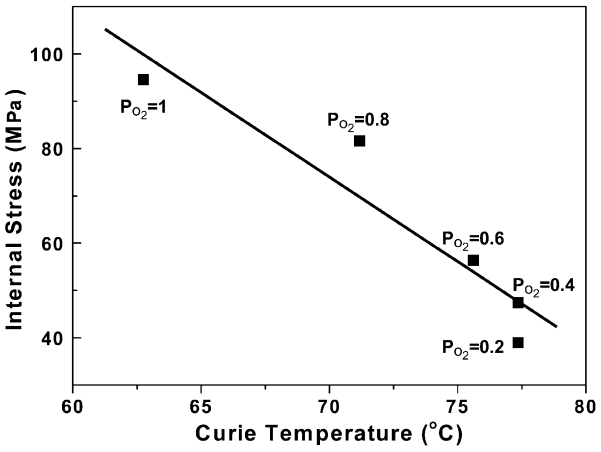

Fig. 7. Relationship between internal stress and Curie temperature.

sintered in different Po_2. Based on the relation, a figure of internal stress vs. Po_2 can be depicted as shown in Fig. 7. The overall tendency revealed that the internal stress increased from 39.0 to 94.5 MPa when Po_2 increased from 0.2 to 1 atm. Because the phase transformation temperature of the samples decreases with respect to the increase of Po_2, the phase transformation temperature is inversely proportional to the internal stress. At this point we can consider a relationship between internal stress and pores since internal stresses can be relieved by pores, which do not constrain grains.[19] As seen in the SEM microstructures (Fig. 1) and relative density (Fig. 2) of samples, higher Po_2 of sintering atmosphere lead to lower porosity, which resulted in higher internal stress. Consequently, the increased Curie temperature as the Po_2 of sintering atmosphere decreased seems to be the result of relaxed internal stresses due to the presence of pores in the microstructure.[8,20]

4. Conclusion

$Sr_{0.5}Ba_{0.5}Nb_2O_6$ ceramics were double-stage sintered in sintering atmospheres with different oxygen partial pressure. The mean grain size of the samples was almost invariant with the Po_2 showing 10.9 μm. Density, transmittance and dielectric constant of the sintered body increased while the Curie temperature decreased as the Po_2 increased. The sample sintered in oxygen, which is a soluble gas in oxides, led to high density. Optical transmittance and dielectric constant were dependent on Po_2. Curie temperature of SBN samples was changed when the samples were sintered in different Po_2. Pores in the microstructure played a major role in relaxation of internal stresses which increased the Curie temperature.

Acknowledgements

This work was supported by grant No. R01-2000-00233 from the Basic Research Program of the Korea Science & Engineering Foundation.

References

1. Glass, A. M., Investigation of the electrical properties of $Sr_{1-x}Ba_xNb_2O_6$ with special reference to pyroelectric detection. *J. Appl. Phys.*, 1969, **40**, 4699–4713.
2. Nagata, K., Yamamoto, Y., Igarashi, H. and Okazaki, K., Properties of the hot-pressed strontium barium niobate ceramics. *Ferroelectrics*, 1981, **38**, 853–856.
3. Ewbank, M. D., Neugaonkar, R. R., Cory, W. K. and Feinberg, J., Photorefractive properties of strontium-barium niobate. *J. Appl. Phys.*, 1987, **62**, 374–380.
4. Xu, Y., *Ferroelectric Materials and Their Applications*. Elsevier Science Publishers, 1991.
5. Kim, M. S., Lee, J. H., Kim, J. J., Lee, H. Y. and Cho, S. H., Microstructure and dielectric characteristics of tungsten bronze structured SBN70 ceramics: effect of Nb_2O_5 content. *J. Eur. Ceram. Soc.*, 2002, **22**, 2107–2113.
6. Lee, H. Y. and Freer, R., Structural stability of strontium barium niobate ceramics. *Fourth Euro Ceramics*, 1995, **55**, 219–226.
7. Huang, W. H., Xu, Z. and Viehland, D., Structure–property relationships in strontium Barium II. Quenching and annealing effects. *Philos. Mag. A*, 1995, **71**, 219–229.
8. Hiroshima, T., Tanaka, K. and Kimura, T., Effects of microstructure and composition on the Curie temperature of lead barium niobate solid solutions. *J. Am. Ceram. Soc.*, 1996, **79**(12), 3235–3242.
9. BallMan, A. A. and Brown, H., The growth and properties of strontium barium metaniobate, $Sr_{1-x}Ba_xNb_2O_6$, a tungsten bronze ferroelectric. *J. Cryst. Growth*, 1967, **1**, 311–314.
10. Guo, R., Bhalla, A. S., Burns, G. and Dacol, F. H., Studies of annealing and quenching of strontium barium niobate (SBN) single crystals: A-site cation ordering–disordering effect. *Ferroelectrics*, 1989, **93**, 397–405.
11. Lee, H. Y. and Freer, R., The mechanism of abnormal grain growth in $Sr_{0.6}Ba_{0.4}Nb_2O_6$ ceramics. *J. Appl. Phys.*, 1997, **81**, 376–382.
12. Brandon, D. and Kaplan, W. D., *Microstructural Characterization of Materials*. J. Wiley, New York, 1999.
13. Lee, W. J. and Fang, T. T., Effect of the strontium:barium ratio and atmosphere on the sintering behavior of strontium barium niobate. *J. Am. Ceram. Soc.*, 1998, **81**, 300–304.
14. Simmons, J. H. and Potter, K. S., *Optical Materials*. Academic Press, San Diego, 2000.
15. Moriga, T., Edwards, D. D. and Mason, T. O., Phase relationships and physical properties of homologous compounds in the zinc oxide—ludium oxide system. *J. Am. Ceram. Soc.*, 1998, **81**, 1310–1316.
16. Cross, L. E., Relaxor Ferroelectrics: An Overview. *Ferroelectrics*, 1994, **151**, 305–320.
17. Trubelja, M. P., Raba, E. and Smith, D. K., A study of positional disorder in strontium barium niobate. *J. Mater. Sci.*, 1996, **31**, 1435–1443.
18. Okazaki, K., Mechanical behavior of ferroelectric ceramics. *Ceram. Bulletin*, 1984, **63**, 1157–1550.
19. Kingery, B. U., *Introduction to Ceramics*. Wiley, New York, 1976.
20. Kimura, T., Miyamoto, S. and Yamaguchi, T., Microstructure, development and dielectric properties of potassium strontium niobate ceramics. *J. Am. Ceram. Soc.*, 1990, **73**, 127–130.